Plant Communications
Research article

CellPress
Partner Journal

The APETALA2–MYBL2 module represses proanthocyanidin biosynthesis by affecting formation of the MBW complex in seeds of *Arabidopsis thaliana*

Wenbo Jiang[1,*], Qinggang Yin[2], Jinyue Liu[2], Xiaojia Su[2], Xiaoyan Han[2], Qian Li[1], Jin Zhang[1] and Yongzhen Pang[1,*]

[1]Institute of Animal Science, Chinese Academy of Agricultural Sciences, Beijing 100193, China

[2]Key Laboratory of Plant Resources and Beijing Botanical Garden, Institute of Botany, Chinese Academy of Sciences, Beijing 100093, China

***Correspondence: Wenbo Jiang (jiangwenbo@caas.cn), Yongzhen Pang (pangyongzhen@caas.cn)**

https://doi.org/10.1016/j.xplc.2023.100777

ABSTRACT

Proanthocyanidins (PAs) are the second most abundant plant phenolic natural products. PA biosynthesis is regulated by the well-documented MYB/bHLH/WD40 (MBW) complex, but how this complex itself is regulated remains ill defined. Here, *in situ* hybridization and β-glucuronidase staining show that *APETALA2* (*AP2*), a well-defined regulator of flower and seed development, is strongly expressed in the seed coat endothelium, where PAs accumulate. AP2 negatively regulates PA content and expression levels of key PA pathway genes. AP2 activates *MYBL2* transcription and interacts with MYBL2, a key suppressor of the PA pathway. AP2 exerts its function by directly binding to the AT-rich motifs near the promoter region of *MYBL2*. Molecular and biochemical analyses revealed that AP2 forms AP2–MYBL2–TT8/EGL3 complexes, disrupting the MBW complex and thereby repressing expression of *ANR*, *TT12*, *TT19*, and *AHA10*. Genetic analyses revealed that AP2 functions upstream of MYBL2, TT2, and TT8 in PA regulation. Our work reveals a new role of AP2 as a key regulator of PA biosynthesis in *Arabidopsis*. Overall, this study sheds new light on the comprehensive regulation network of PA biosynthesis as well as the dual regulatory roles of AP2 in seed development and accumulation of major secondary metabolites in *Arabidopsis*.

Jiang W., Yin Q., Liu J., Su X., Han X., Li Q., Zhang J., and Pang Y. (2024). The APETALA2–MYBL2 module represses proanthocyanidin biosynthesis by affecting formation of the MBW complex in seeds of *Arabidopsis thaliana*. Plant Comm. **5**, 100777.

INTRODUCTION

Proanthocyanidins (PAs), also known as condensed tannins, are the second most abundant plant phenolic polymers after lignins, and they are present in the leaves, bark, fruits, and seeds of many plants (Dixon et al., 2005; Prior and Gu, 2005). PAs provide protection against predation and give flavor and astringency to beverages such as wine, teas, and fruit juices. PAs enhance soil nitrogen retention, prevent pasture bloat, and improve nitrogen nutrition in ruminant livestock, and they have many beneficial effects on human health (Lees, 1992; Dixon et al., 2005; Joanisse et al., 2009). Significant effort has therefore been focused on characterizing the PA biosynthetic pathway in a range of plant species over the last several decades.

In *Arabidopsis*, PAs are synthesized in the innermost cell layer of the testa (chalaza, micropyle, and endothelium), conferring to the mature seed its characteristic brown color (Debeaujon et al., 2003; Pourcel et al., 2005; Lepiniec et al., 2006). Biosynthesis of PAs begins in the micropylar region around 1–2 days after fertilization, and deposition progresses in the endothelium toward the chalaza until around 5–6 days after fertilization (Debeaujon et al., 2003; Lepiniec et al., 2006). The genetics of the PA subpathway, as well as the common flavonoid pathway, have been well studied in *Arabidopsis*, and more than 20 genes have been shown to participate in the early pathway (e.g., *CHS*, *CHI*, *F3H*, and *F3'H*), late pathway (e.g., *DFR*, *ANS*, and *ANR*), and modification, transport, and oxidation (e.g., *TT12*, *TT19*, *AHA10*, and *TT10*) (Xu et al., 2014; Supplemental Figure 1).

The MBW ternary complex, consisting of MYB (TT2 and MYB5), bHLH (TT8, GL3, and EGL3) and WD repeat (TTG1) proteins

Published by the Plant Communications Shanghai Editorial Office in association with Cell Press, an imprint of Elsevier Inc., on behalf of CSPB and CEMPS, CAS.

(Baudry et al., 2004; Lepiniec et al., 2006; Xu et al., 2014), is the classical regulatory complex in the PA pathway. The TT2–TT8–TTG1 complex plays a leading role, and three other MBW complexes (MYB5–TT8–TTG1, TT2–GL3–TTG1, and TT2–GL3–TTG1) are also involved in PA biosynthesis in a tissue-specific manner (Baudry et al., 2004; Xu et al., 2014). The functions of the MBW partners in regulation of PAs and flavonoids are well conserved in plants (Xu et al., 2015). In the MBW complex, MYB proteins bind to the MYB core elements and AC-rich elements of late biosynthetic genes in the PA subpathway, whereas bHLH proteins bind to their E/G-box motifs (Koshino-Kimura et al., 2005; Ryu et al., 2005; Ishida et al., 2007; Kang et al., 2009; Song et al., 2011; Xu et al., 2014; Li et al., 2022). TTG1 stabilizes the interaction between TT2 and TT8, which is crucial for the transcriptional activity of the MBW complex *in planta* (Baudry et al., 2004; Thevenin et al., 2012). Several other regulators also fine-tune the transcriptional activity of MBW complexes by interacting with MYBs or bHLHs to organize or disrupt complex formation (Dubos et al., 2008; Matsui et al., 2008; Appelhagen et al., 2011; Gonzalez et al., 2016). For instance, the TT1 WIP zinc-finger protein, the TTG2 WRKY transcription factor, and the TT16 MADS protein interact with components of the MBW complex to positively regulate PA biosynthesis (Nesi et al., 2002; Sagasser et al., 2002; Appelhagen et al., 2011; Gonzalez et al., 2016; Xu et al., 2017). By contrast, a few other regulators negatively regulate biosynthesis of PAs and other flavonoids; for example, the MADS transcription factor SEEDSTICK inhibits PA accumulation by modifying the chromatin state of key regulatory genes (e.g., *TT8*, *EGL3*, and *TT16*) and *ANR* (Mizzotti et al., 2014). In particular, the R3-MYB protein MYBL2 negatively regulates anthocyanin and PA biosynthesis by interacting with bHLHs (e.g., TT8, GL3, and EGL3) to inhibit formation of the MBW complex (Sawa, 2002; Zimmermann et al., 2004; Dubos et al., 2008; Matsui et al., 2008). However, bioengineering of PAs based on these regulatory mechanisms of the PA pathway in *Arabidopsis* and other plant species has not been successful to date (Nesi et al., 2001; Sharma and Dixon, 2005; Verdier et al., 2012; Li et al., 2016), mainly owing to our limited understanding of PA regulation. Although several components involved in regulation of the MBW complex have been identified and characterized, additional regulators still remain to be discovered in order to advance our understanding of PA biosynthesis.

Here, we show that APETALA2 (AP2) disrupts formation of the MBW complex to repress PA biosynthesis. Overexpression of *AP2* led to a lighter seed color owing to lower PA content in *Arabidopsis* seeds, implying that AP2 represses PA biosynthesis. AP2 binds to the promoter of *MYBL2* to activate its expression. AP2 also interacts with MYBL2 to repress formation of the MBW complex. Genetic analyses showed that AP2 acts upstream of *MYBL2* and the MBW complex in PA regulation. We conclude that AP2 acts as an activator of *MYBL2* to repress PA biosynthesis by disrupting formation of the MBW complex.

RESULTS

AP2 represses PA biosynthesis

In addition to its better-known roles in floral organ identity (Bowman et al., 1989; Kunst et al., 1989) and flowering time (Yant et al., 2010), AP2 also has essential roles in seed development (Jofuku et al., 2005; Ohto et al., 2005) and differentiation of the outer layers of the seed coat (Western et al., 2001). Our previous study showed that the *Arabidopsis ap2-6* mutant displays a darker seed color than the wild type (Jiang et al., 2013), indicating that the *ap2* mutant may accumulate more PAs in the seed coat. To investigate the effect of AP2 on PA accumulation, seeds of the *ap2-5* and *ap2-6* mutants were stained with *p*-dimethylaminocinnamaldehyde (DMACA), a dye that is commonly used for PAs can react with PAs to form a blue to purple stain, and the *ap2-6* mutant exhibited a darker blue color with a higher PA content than the wild type (Figure 1A and 1B and Supplemental Figure 2).

To further examine the effect of AP2 on PA accumulation, we generated various *AP2* overexpression lines (Supplemental Figure 3A and 3B), including *AP2* overexpression plants (*AP2 OE1-3*), *AP2m3* overexpression plants (*AP2m3 OE1-3*), and *AP2m3 Myc* overexpression plants (*AP2m3 Myc OE1-2*). *AP2 OE* indicates overexpression of the native *AP2* gene; because *AP2* is a target gene of miR172, the transcript level of *AP2* is elevated in *AP2 OE*, but AP2 protein abundance is unchanged. *AP2m3 OE1-3* indicates overexpression of a mutant *AP2* gene whose mutations disrupt miR172 base pairing (Supplemental Figure 3A and 3B) without changing the AP2 amino acid sequence (Chen, 2004). Both *AP2* transcript level and AP2 protein abundance are elevated in *AP2m3 OE1-3*, owing to the failure of miR172 to bind to *AP2m3*. *AP2m3 Myc OE1-2* indicates *AP2m3* with an added Myc tag to facilitate coimmunoprecipitation (coIP) assays; like *AP2m3 OE1-3,* it has elevated *AP2* transcript levels and AP2 protein levels.

Seeds of the *AP2m3* and *AP2m3 Myc* lines exhibited a lighter color and significantly lower PA content than the wild type (Figure 1A and 1B). However, seeds of *AP2 OE1-3* showed a phenotype similar to that of the wild type (Figure 1A and 1B). These results indicate that an increase in AP2 protein leads to decreased PA accumulation in the *Arabidopsis* seed coat.

To evaluate whether flavonoid compounds other than PAs are also affected by AP2, we analyzed anthocyanins and flavonols in seedlings or seeds of these lines, but neither anthocyanins nor flavonols were affected in *AP2* knockout or overexpression lines (Supplemental Figure 4), implying that AP2 specifically represses PA accumulation in seeds.

AP2-like miR172-target clade members and miR172 do not affect PA accumulation

AP2-like miR172-target clade members (e.g., *TOE1*, *TOE2*, *TOE3*, *SMZ*, and *SNZ*) have been reported to redundantly regulate flowering time (Yant et al., 2010). To determine whether these clade members also affect PA accumulation, we analyzed their expression in the seed coat during various seed developmental stages. *AP2* showed the highest expression, and *TOE2* was expressed at a higher level than the remaining four genes (Supplemental Figure 5A), suggesting that *TOE2* might affect biosynthesis of PAs that accumulate specifically in the seeds. Phylogenetic analysis showed that AP2 was clustered in the same clade with TOE1 and TOE3 (Supplemental Figure 5B). Their similar expression patterns and close phylogenetic relationships suggested that *TOE1*, *TOE2*,

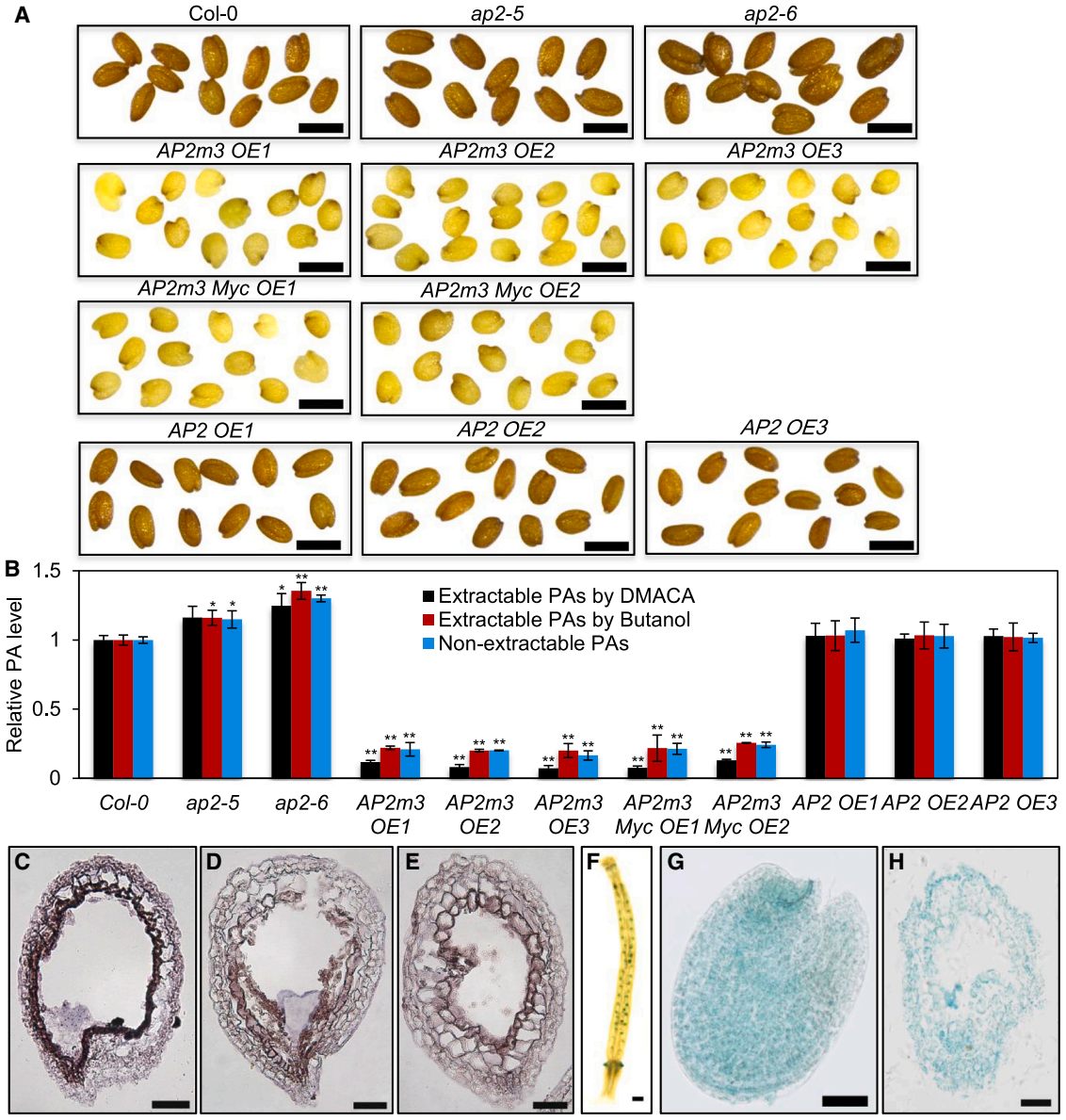

Figure 1. *AP2* represses PA accumulation and is expressed in the seed coat endothelium.

(A) Seed phenotypes of the wild type (Col-0), *ap2* mutants (*ap2-5* and *ap2-6*), and *AP2* overexpression lines (*AP2m3 OE*, *AP2m3 Myc OE*, and *AP2 OE*). Scale bars, 0.5 mm.

(B) Relative PA level in mature seeds of Col-0, *ap2* mutants, and *AP2* overexpression lines. Levels of each type of PA in Col-0 were set to 1.0. Data are presented as mean ± SD, Student's *t*-test ($n = 3$, $^{*}P < 0.05$, $^{**}P < 0.01$).

(C–E) *In situ* hybridization using an *AP2* antisense probe **(C)**, sense control **(D)**, and no-probe control **(E)** in 4-day-old seeds of Col-0. Scale bars, 50 μm.

(F–H) Histochemical analysis of GUS activity generated by proAP2::GUS in 3-day-old siliques **(F)**, seeds without sectioning **(G)**, and seeds with sectioning **(H)**. Scale bars, 200 μm in **(F)** and 50 μm in **(G)** and **(H)**.

and *TOE3* might be involved in PA accumulation. Thus, we also generated transgenic plants overexpressing *TOE1m3*, *TOE2m3*, and *TOE3m3* (Supplemental Figure 3); all harbored a truly silent mutation in the miR172 binding site to ensure elevated transcript levels and protein levels. However, we did not observe a lighter seed color in transgenic seeds overexpressing *TOE1m3*, *TOE2m3*, or *TOE3m3* (Supplemental Figure 6), and their seeds exhibited the same or a similar blue-purple color as wild-type seeds when stained with DMACA (Supplemental Figure 7A). The PA content of these lines was similar to that of the wild type, as determined by quantitative analyses (Supplemental Figure 7B), suggesting that *TOE1*, *TOE2*, and *TOE3* do not affect PA accumulation.

We next asked whether miR172 itself was involved in PA accumulation. Seed color of the transgenic plants overexpressing miR172a was similar to that of the wild type before and after staining with DMACA (Supplemental Figures 3C, 6, and 7), and their PA contents were similar to that of the wild type (Supplemental Figure 7B), indicating that miR172 does not affect PA

accumulation. Taken together, our results clearly indicate that neither *AP2*-like miR172-target clade members nor miR172 affect PA accumulation.

AP2 is expressed in the seed coat endothelium

Because our results indicated a novel function of AP2 in seeds, where PAs accumulate, we analyzed *AP2* expression in early seed development by *in situ* hybridization. We detected a strong signal above background in the endothelium, which is the innermost cell layer of the inner integument (Figure 1C–1E). Some signal above background was also detected in the outer layers of the seed coat and the embryo (Figure 1C–1E), consistent with previous reports that AP2 is a regulator of outer integument differentiation during seed coat development (Western et al., 2001) and that *AP2* is expressed throughout the embryo from the globular stage onward (Wurschum et al., 2006). We next cloned a 5.4-kb fragment upstream of the *AP2* cDNA as the *AP2* promoter (Zhao et al., 2007), fused it to the coding region of β-glucuronidase (GUS), and introduced it into wild-type *Arabidopsis*. This promoter fragment drove GUS expression in the seed coat of 3-day-old seeds (Figure 1F–1H), consistent with the expression pattern of AP2 in the *in situ* hybridization assay. Thus, *AP2* is strongly expressed in the seed coat endothelium, where PAs accumulate, suggesting a direct regulatory role of AP2 in PA accumulation.

AP2 regulates expression of late PA pathway genes and transcriptional regulators

To investigate whether transcript abundance of PA pathway genes is affected by AP2, we examined the expression profiles of 14 biosynthetic genes and 11 transcriptional regulators involved in PA accumulation using available online databases. The expression levels of most genes in the developing *Arabidopsis* seed coat were relatively high at the pre-globular and/or globular developmental stages, decreased dramatically at the heart and/or linear cotyledon stages, and decreased further to very low levels at the mature green stage. However, *AP2* was constantly expressed at a high level throughout seed development (Supplemental Figures 5A and 8).

We then measured the relative transcript abundance of all known PA pathway genes in developing seeds (4 days post pollination) by qPCR. In the *AP2m3* overexpression line, relative transcript levels of late pathway genes (e.g., *DFR*, *ANS*, *ANR*, *TT12*, *TT19*, and *AHA10*) decreased significantly compared with the wild type. Expression of *ANR*, *TT12*, *TT19*, and *AHA10* increased in the *ap2-6* mutant compared with the wild type (Figure 2A), indicating that AP2 negatively regulates expression of these genes. Among the 11 transcriptional regulatory genes analyzed, *TT2* was significantly inhibited by AP2, whereas *MYBL2* was activated by AP2 (Figure 2B). These results indicated that AP2 represses PA accumulation by specifically regulating the expression of late pathway genes (e.g., *DFR*, *ANS*, *ANR*, *TT12*, *TT19*, and *AHA10*) and specific transcriptional regulators (*TT2* and *MYBL2*).

AP2 activates *MYBL2* transcription by binding to its promoter

To explore how AP2 regulates the PA pathway genes, we performed an *in vitro* transcription assay in *Arabidopsis* leaf protoplasts to determine the effects of *AP2m3* co-expression on transactivation of a reporter gene (firefly luciferase) driven by the promoters of the PA pathway genes. Surprisingly, we found that *AP2m3* activated expression of the reporter gene driven by the *MYBL2* promoter by 3.5-fold but did not activate expression of the other 24 genes (Figure 3A). This result suggested that AP2 positively and uniquely regulates the expression of *MYBL2* directly, consistent with its expression changes in the *ap2* mutant and *AP2m3 OE* lines (Figure 2B). We also examined the expression level of *MYBL2* during seed development and found that *MYBL2* expression was reduced in the *ap2-6* mutant compared with the wild type during seed development (Supplemental Figure 9), indicating that AP2 activates *MYBL2* expression.

A previous study showed that AP2 directly regulates *AGAMOUS* (*AG*), a C-class floral organ identity gene, by binding to the AT-rich motif (TTTGTT or AACAAA) in young flowers (Dinh et al., 2012). Thus, AP2 may directly activate *MYBL2* by binding to its AT-rich motif(s). We identified five AT-rich motifs (M1–M5) within/near the promoter region of *MYBL2* (Figure 3B) and mutated the native AT-rich motifs (m1–m5 and different combinations) to CCCCCC to examine their effects on *MYBL2* expression. AP2 failed to activate *MYBL2* expression in *in vitro* transcription assays whenever M5 (m5) was mutated (Figure 3C). By contrast, mutation of motifs M1–M4 (m1–m4) in different combinations had no significant effect on *MYBL2* expression (Figure 3C). These results indicate that AP2 binds to the M5 motif to activate *MYBL2* expression.

We next performed a chromatin IP (ChIP) assay to test whether AP2 could bind to the promoter of *MYBL2 in vivo*. A transgenic *Arabidopsis* line overexpressing *AP2m3 Myc* was used for ChIP analysis, along with the wild type as a negative control. AP2m3 Myc bound to the M5F/R region containing the AT-rich M5 motif but not to other regions (Figure 3D), consistent with the mutation analysis of the AT-rich motifs (Figure 3C). These results indicate that AP2 specifically binds to the AT-rich M5 motif of *MYBL2*.

AP2 interacts with MYBL2 *in vivo*

Yeast two-hybrid assays were used to determine whether any of the 11 transcriptional regulators of the PA pathway interact with AP2. Yeast cells co-transformed with AP2-BD and MYBL2-AD grew well on selection medium, and those with AP2-BD and TT2-AD and with AP2-BD and MYB5-AD grew slowly (Supplemental Figure 10). Yeast cells co-transformed with AP2-BD and eight other transcriptional regulators did not grow at all (Supplemental Figure 10). These results indicated that AP2 can physically interact with MYBL2, TT2, and MYB5 in yeast. The *in vivo* interactions between AP2 and MYBL2, AP2 and TT2, and AP2 and MYB5 were examined using bimolecular fluorescence complementation (BiFC) and coIP assays. Co-expression of AP2-N terminal yellow fluorescence protein with MYBL2-CYFP in leaves of *Nicotiana benthamiana* produced intense yellow fluorescent protein (YFP) fluorescence, whereas no YFP signal was observed when AP2-N terminal yellow fluorescence protein was co-expressed with TT2-CYFP or MYB5-CYFP (Supplemental Figure 11), confirming that AP2 interacts only with MYBL2 *in vivo*. Consistent with this finding, FLAG-tagged MYBL2 was immunoprecipitated with an antibody against c-Myc when c-Myc-tagged AP2m3 was co-expressed with

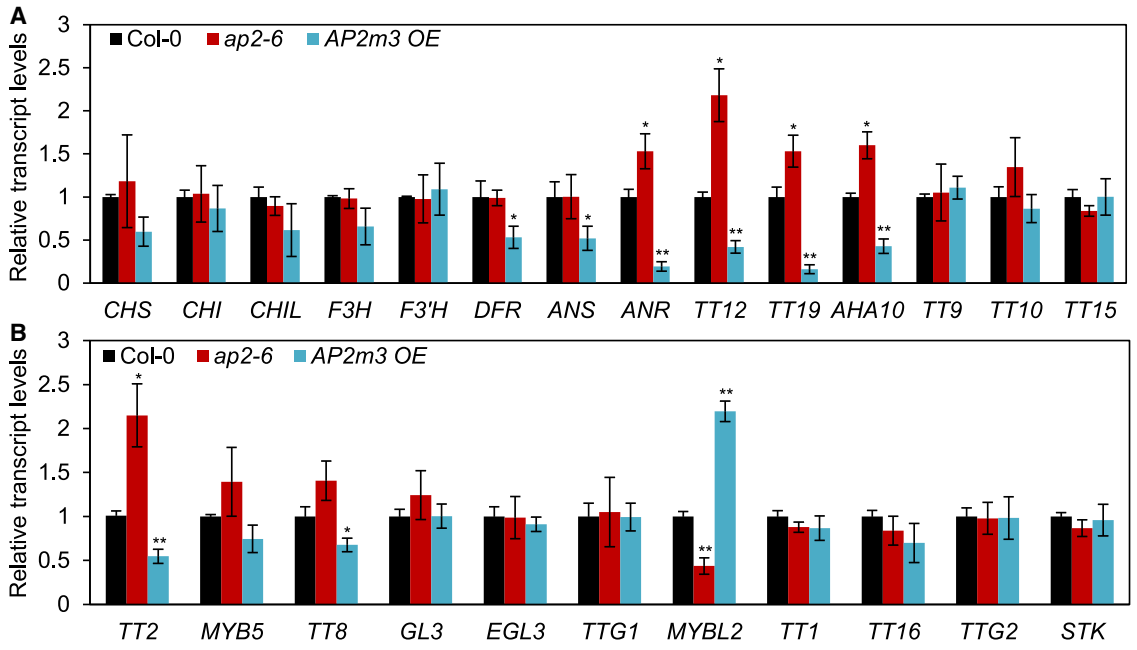

Figure 2. AP2 represses PA accumulation by regulating the expression of late biosynthetic genes and transcriptional regulator genes.

(A and B) Relative transcript levels of 14 structural genes **(A)** and 11 transcriptional regulator genes **(B)** in 4-day-old siliques of Col-0, *ap2-6* mutant, and *AP2m3 OE* lines. The transcript level of each gene in Col-0 was set to 1.0. Data are presented as mean ± SD, Student's *t*-test ($n = 3$, $^{*}P < 0.05$, $^{**}P < 0.01$).

FLAG-tagged MYBL2 in *N. benthamiana* leaves (Figure 4A). Taken together, these results demonstrate that AP2 physically interacts with MYBL2 *in vivo*.

AP2 represses transcriptional activity of the MBW complex by interacting with MYBL2

Previous studies have used yeast two-hybrid assays to show that MYBL2 negatively regulates anthocyanin and PA biosynthesis by interacting with TT8, GL3, and EGL3, thereby inhibiting the transcriptional activity of the MBW complex (Sawa, 2002; Zimmermann et al., 2004; Dubos et al., 2008; Matsui et al., 2008). In this study, we performed BiFC and coIP assays to further confirm the direct interactions of MYBL2 with TT8, GL3, and EGL3 (Figure 4B–4D and 4G and Supplemental Figure 12). Because MYBL2 also interacts with AP2, as shown above, we hypothesized that MYBL2 could interact simultaneously with AP2 and the TT8/GL3/EGL3 complex. To test this hypothesis, we generated different truncated forms of MYBL2 and tested their interactions with AP2 in yeast two-hybrid assays (Supplemental Figure 13A). AP2 bound to C-terminal truncations of MYBL2 (Figure 4E; Supplemental Figure 13A), and TT8 bound to N-terminal truncations of MYBL2 (Figure 4F), as further confirmed by BiFC assays (Figure 4G). Yeast two-hybrid assays also showed that GL3 bound to C-terminal truncations of MYBL2 (Supplemental Figure 13C) and EGL3 to N-terminal truncations of MYBL2 (Supplemental Figure 13D). These results indicate that MYBL2 interacts simultaneously with AP2 and TT8/EGL3 at the C terminus and N terminus, respectively. Additional coIP assays showed that c-Myc-tagged AP2m3 was immunoprecipitated with an antibody against hemagglutinin (HA) when c-Myc-tagged AP2m3 and FLAG-tagged MYBL2 were co-expressed with HA-tagged TT8/HA-tagged EGL3 (Figure 5A and 5B), whereas c-Myc-tagged AP2m3 was not immunoprecipitated when they were co-expressed with FLAG-tagged MYBL2 and HA-tagged GL3 (Figure 5C). These results indicate that MYBL2 bridges AP2 and TT8/EGL3 to form the AP2–MYBL2–TT8 or AP2–MYBL2–EGL3 complex.

MYBL2 has been shown to inhibit *ANR* expression by repressing the MBW complex (TT2–TT8–TTG1 complex) (Thevenin et al., 2012). We hypothesized that AP2 inhibits the transcription of the MBW complex by interacting with MYBL2. To test this hypothesis, a transient transactivation system was used to test the effect of simultaneous and constitutive expression of *AP2* and *MYBL2* on expression of *proANR*:*luciferase* in the presence or absence of the TT2–TT8–TTG1 complex. It was clear that the presence of the TT2–TT8–TTG1 complex resulted in higher activation activity than the presence of one or two genes (Figure 5D). Quantification of luciferase activity showed that the presence of *MYBL2* significantly decreased luciferase activity of the TT2–TT8–TTG1 complex. The presence of *AP2m3* with the TT2–TT8–TTG1 complex did not change its activity compared with the TT2–TT8–TTG1 complex alone. By contrast, the presence of both *MYBL2* and *AP2m3* with the TT2–TT8–TTG1 complex led to even lower activity than that observed for the TT2–TT8–TTG1 complex with *MYBL2* (Figure 5D). This result suggests that MYBL2 is required for AP2-repressed transcriptional activity of the TT2–TT8–TTG1 complex for activation of *ANR*. Taken together, these results demonstrate that AP2 represses the transcriptional activity of the TT2–TT8–TTG1 complex by interacting with MYBL2.

AP2 functions upstream of *MYBL2* and the MBW complex in PA biosynthesis

The results above showed that AP2 plays key roles in regulating PA biosynthesis via MYBL2 and the MBW complex. We next

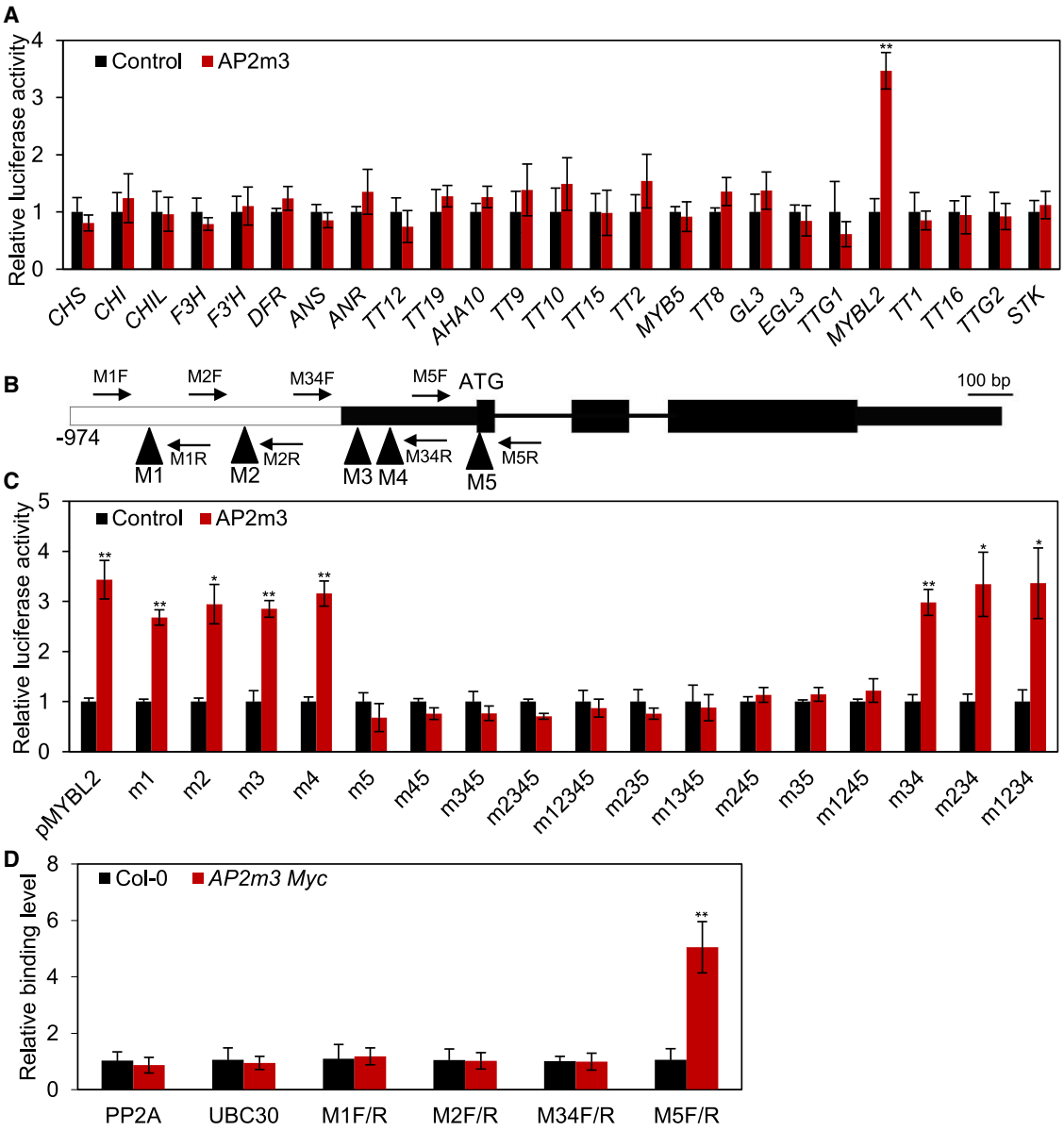

Figure 3. *AP2* activates the expression of *MYBL2* by binding to AT-rich motifs.

(A) *AP2m3* was co-expressed with a reporter gene driven by the promoters of PA pathway genes in *Arabidopsis* leaf protoplasts. Induction of the reporter gene was measured by assaying firefly luciferase activity. Luciferase activity of the control without *AP2m3* was set to 1.0.

(B) The position of five AT-rich motifs (TTTGTT or AACAAA) (M1, −751 to −756; M2, −555 to −560; M3, −256 to −261; M4, −233 to −238; and M5, +4 to +9) located in/near the promoter, coding sequence, and 3′ UTR of *MYBL2*. Black triangles indicate AT-rich motifs. Bars, 100 bp.

(C) *AP2m3* was co-expressed with a reporter gene driven by the native promoter or mutated promoters of *MYBL2* in *Arabidopsis* leaf protoplasts (m indicates that the native AT-rich motif was mutated to CCCCCC). Luciferase activity in the control without *AP2m3* was set to 1.0.

(D) Chromatin immunoprecipitation (ChIP) assay of the *MYBL2* promoter. One transgenic line (*AP2m3 Myc OE-1*) overexpressing *AP2m3 Myc* and Myc antibody were used for the ChIP assay, with the wild type (Col-0) as a negative control. *PP2A* and *UBC30* were included as controls. Three independent experiments were carried out with similar results. Data are presented as mean ± SD, Student's *t*-test ($n = 3$, $^*P < 0.05$, $^{**}P < 0.01$).

investigated their genetic interactions using overexpression and mutant lines. Overexpression of *AP2m3* in the *mybl2* mutants resulted in seed color and PA content similar to those of the *mybl2* mutants (Figure 6A, 6B, and 6D). Overexpression of *MYBL2* in the *ap2-6* mutant led to seed color and PA content similar to those of the *MYBL2* overexpression plants (Figure 6A, 6B, and 6D), suggesting that *AP2* acts upstream of *MYBL2*. Additional genetic studies showed that the double mutants *ap2-6/tt2* and *ap2-6/tt8* exhibited the typical pale yellow seed color of *tt2* and *tt8* mutants, consistent with their PA content (Figure 6C and 6E), suggesting that *AP2* acts upstream of the MBW complex. *AP2* thus functions genetically upstream of *MYBL2* and the MBW complex to regulate PA biosynthesis.

DISCUSSION

Arabidopsis AP2 is a multifunctional gene expressed in the sepal, petal, stamen, and carpel and is associated with flower organ

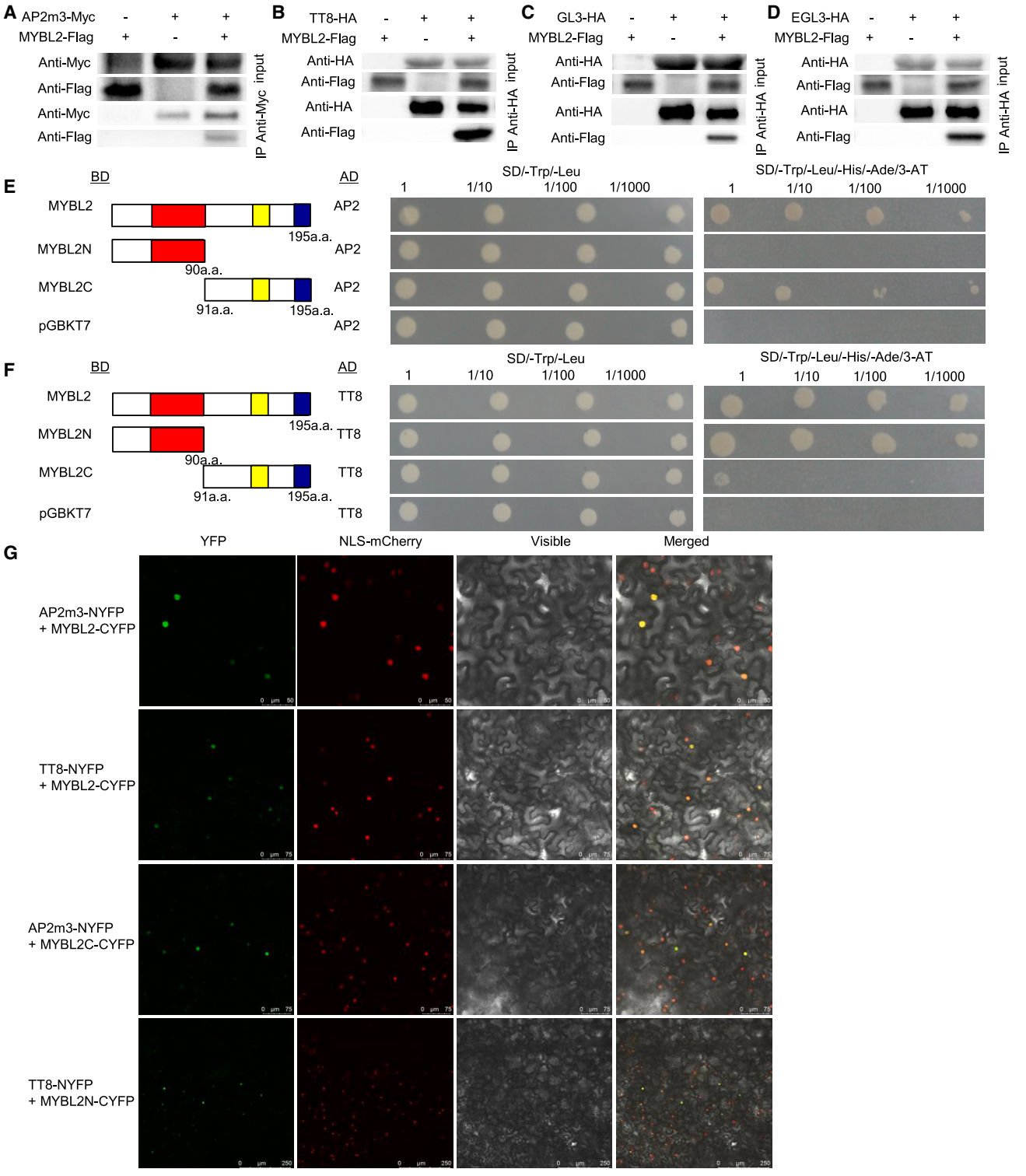

Figure 4. AP2 interacts with MYBL2, and MYBL2 interacts with TT8, GL3, and EGL3.

(A–D) CoIP analysis of AP2 interaction with MYBL2, and MYBL2 interaction with TT8, GL3, and EGL3.

(A) AP2m3-Myc and MYBL2-FLAG were detected with anti-Myc and anti-FLAG antibodies, respectively.

(B–D) TT8-HA **(B)**, GL3-HA **(C)**, and EGL3-HA **(D)** and MYBL2-FLAG were detected with anti-HA and anti-FLAG antibodies, respectively.

(E and F) Yeast two-hybrid assays between different truncations of MYBL2 and AP2 or TT8. Left: vectors containing proteins fused with BD or AD. Center: yeast cells containing BD and AD were diluted with sterile demineralized water at ratios of 1:10, 1:100, and 1:1000 on SD/−Trp/−Leu medium at 30°C for 3 days. Right: the above diluted yeast cells grown on SD/−Trp/−Leu/−His/−Ade medium with 2 mM 3-amino-1,2,4-triazole at 30°C for 7 days.

(G) Protein interaction analysis of different truncations of MYBL2 and AP2 or TT8 in leaves of *N. benthamiana* with a nuclear localization marker (nuclear localization signal-mCherry).

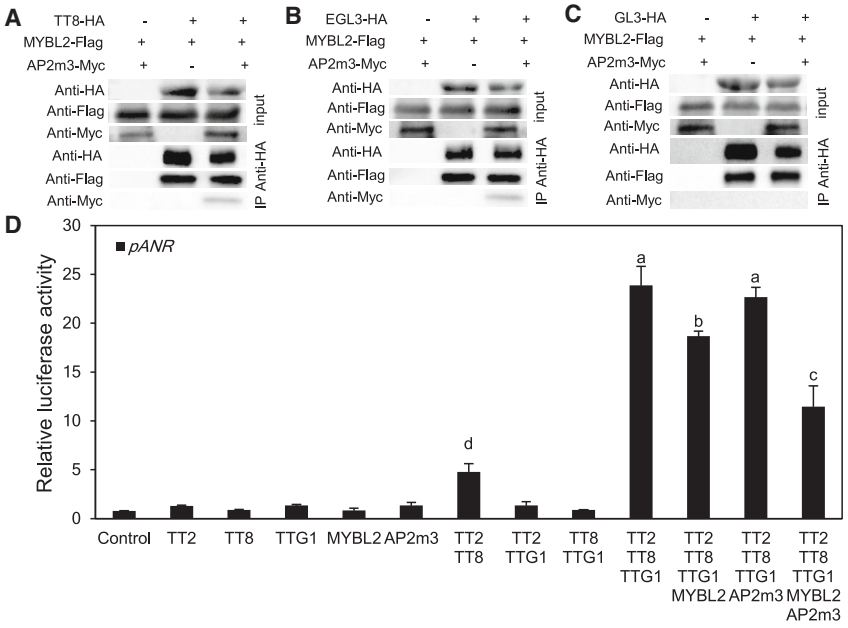

Figure 5. AP2 interacts with MYBL2 and TT8 or EGL3 to form the AP2–MYBL2–TT8/EGL3 complex, thus repressing transcriptional activity of the MBW complex.

(A–C) CoIP analysis of AP2 interaction with MYBL2, TT8, GL3, and EGL3. AP2m3-Myc, MYBL2-FLAG, and TT8-HA **(A)**, EGL3-HA **(B)**, and GL3-HA **(C)** were detected with anti-Myc, anti-FLAG, and anti-HA antibodies, respectively.

(D) AP2 represses transcriptional activity of the MBW complex by interacting with MYBL2. AP2 enhances MYBL2-mediated transcriptional repression activity of the MBW complex, as demonstrated by analysis of *proANR* activity. Compared with that of protoplasts co-transfected with *proANR:luciferase*, *TT2*, *TT8*, *TTG1*, and *MYBL2*, luciferase activity of protoplasts co-transfected with *proANR:luciferase, TT2, TT8, TTG1, MYBL2,* and *AP2m3* was reduced. Values that differ at $P < 0.05$ are labeled with different letters according to one-way ANOVA with post hoc Tukey's Honestly Significant Difference.

identity (Bowman et al., 1989, 1991; Kunst et al., 1989; Drews et al., 1991; Jofuku et al., 1994; Wollmann et al., 2010; Krogan et al., 2012). *AP2* also functions in stem cell maintenance in the shoot apical meristem (Wurschum et al., 2006), control of floral stem cells (Aukerman and Sakai, 2003; Chen, 2004; Yumul et al., 2013; Liu et al., 2014; Huang et al., 2017), and regulation of flowering time (Mathieu et al., 2009; Yant et al., 2010; O'Maoileidigh et al., 2021). In addition, *AP2* controls fruit and seed development (Jofuku et al., 1994; Ripoll et al., 2011) and mediates seed size by affecting embryo, endosperm, and seed coat development (Jofuku et al., 2005; Ohto et al., 2005; 2009). *AP2* is essential for differentiation of the outer layers of the seed coat (Western et al., 2001), and the *ap2-6* mutant exhibits a darker seed color (Jiang et al., 2013). The seed color of *Arabidopsis* is mainly contributed by PAs; therefore, it is important to clarify whether *AP2* also regulates PA biosynthesis in the seed coat.

We found that the *ap2-6* mutant with a much darker seed color accumulates more PA than the wild type (Figure 1A and 1B and Supplemental Figure 2). To further determine the effect of *AP2* on PA accumulation, we generated *AP2* overexpression lines with higher *AP2* RNA abundance than the wild type (Supplemental Figure 3B). However, overexpression of *AP2* resulted in a brown seed color and a PA content similar to those of the wild type (Figure 1A and 1B). A previous study showed that *AP2* RNA abundance was elevated in *AP2* overexpression plants but that AP2 protein abundance was not increased compared with the wild type owing to the presence of miR172, a translational repressor that inhibits production of AP2 protein at the translational level (Chen, 2004). Therefore, although *AP2* RNA abundance is elevated in the *AP2 OE* lines, AP2 protein abundance may not be elevated, and PA accumulation may not be affected. To eliminate the effect of miR172 on AP2, we generated *AP2m3* overexpression plants that harbor a truly silent mutation in the miR172 binding sites (Chen, 2004). As expected, the *AP2m3* overexpression plants had a pale yellow seed color and a much lower PA content (Figure 1A and 1B). Results from *in situ* hybridization and GUS staining showed that *AP2* was strongly expressed in the seed coat endothelium, where PAs accumulate (Figure 1C–1H).

The *AP2*-like miR172-target clade members play a redundant role in flowering time, in part through tissue-specific expression of particular members (Yant et al., 2010). We determined whether they also play a redundant role in PA accumulation. Their transcript levels in the seed coat and phylogenetic relationships (Supplemental Figure 5) suggested that *TOE1*, *TOE2*, and *TOE3* might be involved in PA accumulation. However, on the basis of genetic analyses in *Arabidopsis*, the *AP2*-like miR172-target clade members are not involved in PA accumulation like *AP2*, although they play a redundant role in flowering time (Supplemental Figures 3, 6, and 7). This result indicates that the miR172-target clade members have overlapping and independent roles during the same or different developmental processes.

AP2 functions not only as a direct repressor but also as a transcriptional activator in the regulation of *SOC1*, *AG*, and *AGL15* during flower development (Yant et al., 2010; Dinh et al., 2012; Krogan et al., 2012). This is also the case for its regulation of PA biosynthesis. On the one hand, AP2 negatively regulates expression of late PA biosynthetic genes and the regulatory gene *TT2*. On the other hand, AP2 activates expression of *MYBL2* (Figure 2A and 2B), and AP2 binds to the AT-rich motif of *MYBL2* to directly activate its transcription (Figure 3). Our results suggest that AP2 acts as a transcriptional activator to directly promote expression of *MYBL2*, which in turn disrupts formation of MBW complexes to repress PA accumulation.

Interestingly, besides regulating *MYBL2* at the transcriptional level, AP2 can also interact with MYBL2 at the protein level (Figure 4A, 4E, and 4G and Supplemental Figures 10 and 11). AP2 interacts with TOE3 to regulate *Arabidopsis* floral

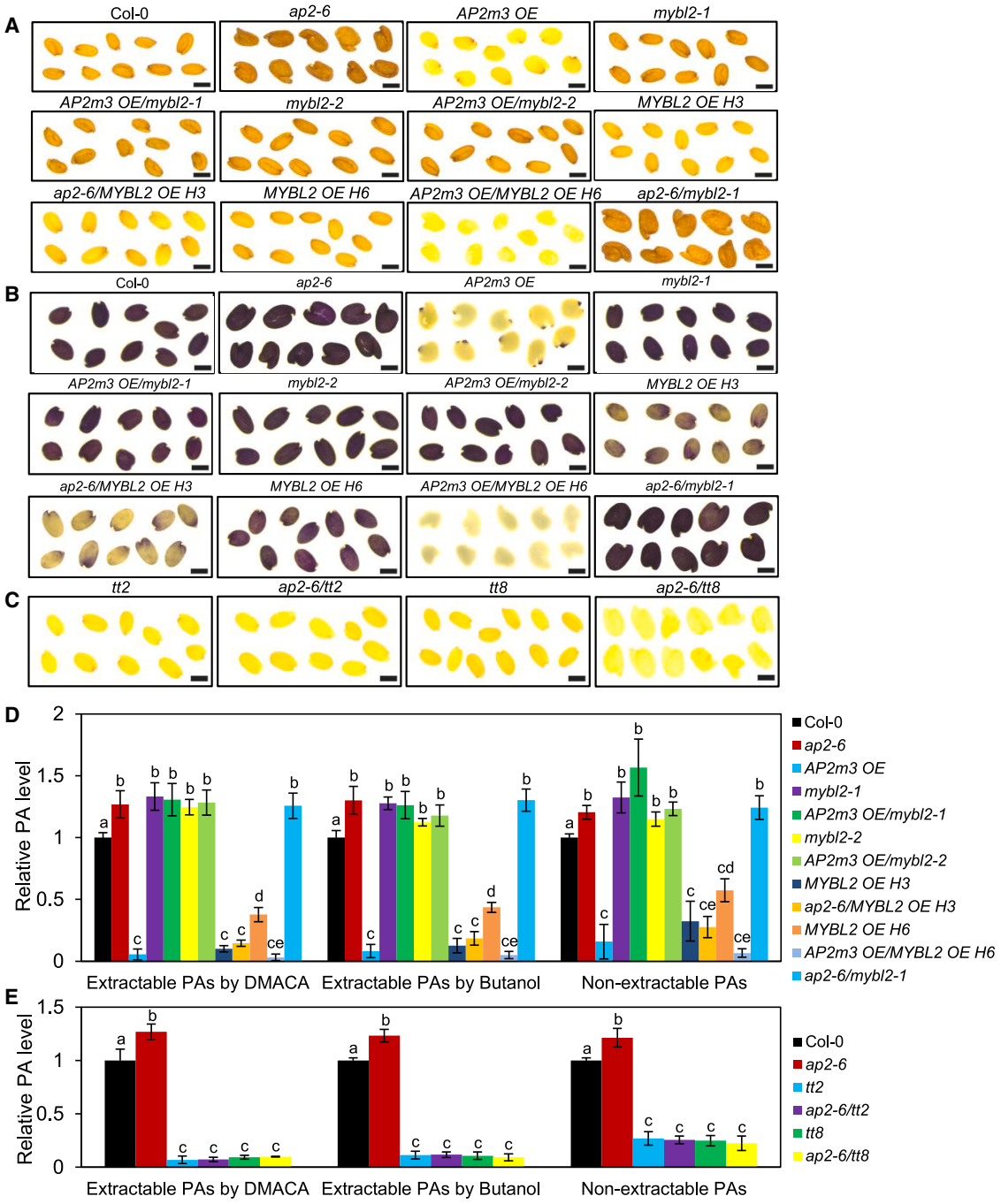

Figure 6. *AP2* acts upstream of *MYBL2* and the MBW complex, and *AP2* repression of PA biosynthesis is dependent on its downstream gene *MYBL2*.

(A) Seed phenotypes of Col-0, *ap2-6*, *mybl2-1*, *mybl2-2*, *AP2m3 OE*, *MYBL2 OE*, and their double mutants. Scale bars, 0.4 mm.

(B) Mature seeds were stained with DMACA for 5 days. Scale bars, 0.4 mm.

(C) Seed phenotypes of *tt2*, *tt8*, and their double mutants with *ap2-6*. Scale bars, 0.4 mm.

(D and E) Relative PA levels in mature seeds. Levels of each type of PA in Col-0 were set to 1.0. Data are presented as mean ± SD. Values that differ at $P < 0.05$ are labeled with different letters according to one-way ANOVA with post hoc Tukey's Honestly Significant Difference.

patterning (Jung et al., 2014), and AP2 represses the expression of its target genes *AG*, *AP3*, *PI*, and *SEP3* by physically recruiting the co-repressor TOPLESS and the histone deacetylase HDA19 (Krogan et al., 2012). Previous studies have shown that MYBL2 also interacts with TT8, GL3, and EGL3 in yeast and possibly inhibits formation of the MBW complex *in planta* (Sawa, 2002; Zimmermann et al., 2004; Dubos et al., 2008; Matsui et al., 2008). Until now, no evidence has shown direct protein interactions between MYBL2 and bHLHs (TT8, GL3, and EGL3) *in planta*. Our present studies confirmed direct *in vivo* interactions

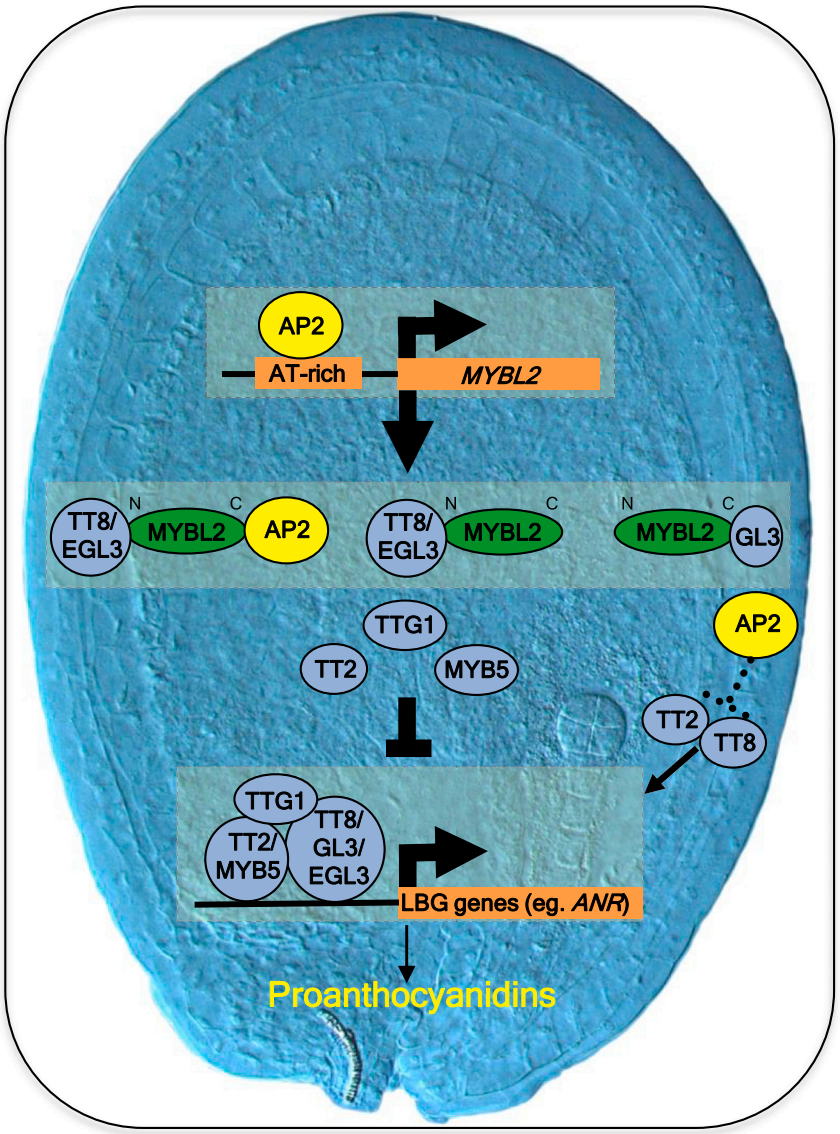

Figure 7. A proposed working model for regulation of PA biosynthesis by AP2 through *MYBL2*.

AP2 regulates the PA pathway at two levels. At the transcript level, AP2 directly activates expression of *MYBL2* by binding to an AT-rich element in the *MYBL2* promoter, disrupting formation of the MBW complex by directly interacting with TT8, GL3, or EGL3. At the protein level, AP2 interacts with MYBL2 to promote formation of the AP2–MYBL2–TT8 or AP2–MYBL2–EGL3 complex, which disrupts formation of the MBW complex and in turn represses expression of late biosynthetic gene genes (e.g., *ANR*), finally inhibiting PA accumulation.

between MYBL2 and TT8/GL3/EGL3 (Figure 4C, 4D, 4F, and 4G and Supplemental Figure 12), showing that MYBL2 interacts simultaneously with AP2 and TT8/GL3/EGL3 at different protein termini (Figure 4E and 4F and Supplemental Figure 13). CoIP assays further confirmed that MYBL2 can interact with AP2 and TT8/EGL3 simultaneously *in planta* (Figure 5A and 5B).

Previous studies have shown that the MBW complex transcriptionally activates late biosynthetic genes to regulate PA biosynthesis (Xu et al., 2014). In addition, when *MYBL2* is co-expressed with the TT2–TT8–TTG1 complex, the transcript level of *ANR* is significantly repressed owing to the interaction of MYBL2 with TT8, which disrupts formation of the TT2–TT8–TTG1 complex (Thevenin et al., 2012). Using transient expression assays, we provided new evidence that AP2 represses *ANR* expression by interacting with MYBL2 to repress the transcriptional activity of the MBW (TT2–TT8–TTG1) complex (Figure 5D). Because the MBW complex activates expression of late biosynthetic genes (e.g., *ANR*, *TT12*, and *TT19*) in a similar manner (Xu et al., 2014), we reason that expression of the other late biosynthetic genes is also repressed similarly by AP2.

Taken together, our results suggest that AP2 regulates the PA pathway at two levels. At the transcript level, AP2 activates expression of *MYBL2* by binding to an AT-rich motif, disrupting the formation of the MBW complex by directly interacting with TT8, GL3, or EGL3. At the protein level, AP2 interacts with MYBL2 to promote formation of the AP2–MYBL2–TT8/EGL3 complex, which disrupts formation of the MBW complex and in turn represses expression of PA biosynthetic genes for PA accumulation (Figure 7). In addition, the possibility that AP2 regulates PA biosynthesis via *TT2* (Figure 7), which was significantly inhibited by AP2 at the transcriptional level (Figure 2B), cannot be excluded.

The dual roles played by AP2 in modulating MYBL2 represent a more efficient regulation of PA biosynthesis. Specifically, AP2 activates *MYBL2* transcription to produce more MYBL2 protein, which further increases the level of the AP2–MYBL2 complex, more efficiently promoting formation of the AP2–MYBL2–TT8/EGL3 complex and inhibiting formation of the MBW complex.

Several regulatory proteins involved in mediating the accumulation of anthocyanins/PAs either disrupt or promote formation of the MBW complex. For example, TT1 interacts with TT2 and acts synergistically with the MBW complex to promote PA biosynthesis (Sagasser et al., 2002; Appelhagen et al., 2011), and TTG2 promotes PA accumulation by interacting with TTG1 (Gonzalez et al., 2016). Although these proteins interact with members of the MBW complex, they do not disrupt formation of the MBW complex. However, MYBL2 represses PA and anthocyanin accumulation by interacting with TT8/GL3/EGL3, which also disrupts formation of the MBW complex (Dubos et al., 2008; Matsui et al., 2008). CAPRICE, another R3-MYB transcription factor, regulates anthocyanin accumulation by interacting with PAP1 or PAP2, which disrupts formation of the MBW

complex (Zhu et al., 2009). SPL9 negatively regulates PA biosynthesis by interacting with PAP1, which inhibits formation of the MBW complex (Gou et al., 2011). The JASMONATE-ZIM DOMAIN proteins in the jasmonate signaling pathway interact with bHLH (TT8, GL3, and EGL3) and MYB (PAP1), thereby disrupting formation of the MBW complex and repressing anthocyanin accumulation (Qi et al., 2011). These proteins interact with members of the MBW complex, disrupting its formation. In this study, AP2 was shown to repress PA biosynthesis through protein interactions that disrupt formation of the MBW complex, but unlike CAPRICE, SPL9, or JASMONATE-ZIM DOMAIN proteins, AP2 did not directly interact with members of the MBW complex. Instead, AP2 was shown to interact with an intermediary, MYBL2, to form the AP2–MYBL2–TT8/EGL3 complex, which disrupts formation of the MBW complex. By contrast, DELLA proteins in the gibberellic acid signaling pathway interact with MYBL2, leading to release of bHLHs (TT8, GL3, or EGL3) and subsequently to formation of the MBW complex (Xie et al., 2016). Although AP2 and DELLA proteins all interact with MYBL2, they regulate formation of the MBW complex in an opposite manner. Whether AP2 is associated with DELLA proteins and whether *AP2* orthologs possess the same functions in PA biosynthesis in other plant species are interesting topics for further exploration. Nevertheless, the present study provides new insights into the function of the AP2–MYBL2–MBW cascade in the regulation of PA biosynthesis.

METHODS

Plant materials and growth conditions

The *ap2-5* (CS6239) and *ap2-6* (CS6240) mutants used in the present study have been described previously (Jiang et al., 2013). The *Arabidopsis* transfer DNA insertion mutant lines *mybl2-1* (SALK_107780) and *mybl2-2* (SALK_126807) were obtained from the Arabidopsis Biological Resource Center (The Ohio State University, Columbus, OH, USA). Two *MYBL2* overexpression lines (*MYBL2 OE H3* and *MYBL2 OE H6*) have been described previously (Dubos et al., 2008). All mutants and transgenic *Arabidopsis* plants were in the Columbia-0 background.

For DMACA staining and analyses of PA, flavonol, and anthocyanin content, *Arabidopsis* plants were grown as described previously (Jiang et al., 2015) with minor modifications. For measurement of leaf flavonol content, the plants were grown in a tissue culture room at 22°C under constant light (100 μmol photons m^{-2} s^{-1}) for 6 days.

Plasmid construction and *Arabidopsis* transformation

For generation of transgenic *Arabidopsis* overexpressing *AP2*, the *AP2* open reading frame (ORF) was amplified and cloned into pENTR/SD/D-TOPO (Invitrogen, Carlsbad, CA, USA). For generation of transgenic *Arabidopsis* overexpressing *AP2m3*, *TOE1m3*, *TOE2m3*, or *TOE3m3*, their nucleotide sequences were mutated to the miR172-resistant version without changing their encoded amino acid sequences and then cloned into pENTR/SD/D-TOPO. For generation of transgenic lines overexpressing miR172a, a previously described fragment of miR172a (Schwab et al., 2005) was cloned into pENTR/SD/D-TOPO. All entry vectors were confirmed by sequencing and then recombined into the Gateway plant transformation vector pB2GW7; pENTR-AP2m3 was also recombined into the Gateway plant transformation vector CTAPi-GW-3×Myc.

Constructs used for plant transformation were delivered into the *Agrobacterium tumefaciens* strain GV3101 by the freeze–thaw method. Transgenic plants were generated by the floral dip method (Clough and Bent, 1998), and seeds were selected on Murashige and Skoog medium supplemented with 10 μg/mL glufosinate ammonium.

In situ hybridization and GUS staining

Four-day-old seeds were isolated from siliques of the wild type (Col-0),fixed in formaldehyde:glacial acetic acid:ethanol solution (1:1:18, by volume), and placed under a vacuum on ice 4 times for 30 min each time. Samples were then incubated at 4°C overnight. After dehydration in an ethanol series, 100% ethanol was replaced by xylene, and the sample was embedded in Paraplast Plus (Sigma). Paraplast sections (8-μm thick) were applied to Poly-Prep slides (Sigma) and incubated at 42°C for 2 days before hybridization. A digoxigenin-labeled antibody was used for *in situ* hybridization, and immunological detection was performed as described previously (Kouchi and Hata, 1993).

For GUS staining, the 5.4-kb fragment upstream of the *AP2* cDNA was cloned as the *AP2* promoter as described previously (Zhao et al., 2007). The promoter fragment was fused to the *GUS* reporter gene and then introduced into wild-type *Arabidopsis*. Three-day-old seeds were isolated from the transgenic lines, and GUS staining was carried out as described in our previous study (Jiang et al., 2015). After dehydration in an ethanol series, 100% ethanol was replaced with xylene, and the sample was embedded in Paraplast Plus (Sigma). Paraplast sections (8-μm thick) were applied to Poly-Prep slides (Sigma).

Gene expression analysis by qPCR

Total RNA was extracted with the Eastep Super Total RNA Extraction Kit (Promega, Madison, WI, USA) according to the manufacturer's instructions. The first-strand cDNA was synthesized using Trans Script One-Step gDNA Removal and cDNA Synthesis SuperMix (TransGen Biotech, Beijing, China). Quantitative RT–PCR was carried out using 2× RealStar Green Fast Mixture (GeneStar, Shanghai, China) and an ABI 7500 Real-Time Detection System (Applied Biosystems, Foster City, CA, USA). The *UBQ10* gene was used as a housekeeping gene. The primer sequences used in this study are listed in Supplemental Table 1. The reactions were carried out as follows: 94°C for 30 s, followed by 40 cycles of 94°C for 5 s and 60°C for 34 s. Data were calculated from biological triplicates with technical triplicates.

Analyses of PAs, flavonols, and anthocyanins

Analyses of PAs, flavonols, and anthocyanins were performed as described previously (Jiang et al., 2015) with minor modifications. For analysis of PAs, 10 μg of finely powdered dry seeds was extracted three times with 0.5 ml extraction buffer (70% acetone with 0.5% acetic acid). For analysis of flavonols, a fine powder of 10 μg dry weight was extracted with 500 μl 80% methanol overnight; the extract was hydrolyzed with the same amount of 3 N HCl at 70°C for 40 min, and then the same amount of methanol was added. Flavonol aglycones were

analyzed in 100-μl samples on an HPLC 1260 instrument (Agilent Technologies, Santa Clara, CA, USA). For analysis of anthocyanins, 20 μg of fine powder was extracted with 500 μl extraction buffer (80% methanol with 0.1% hydrochloric acid). The contents of PAs, flavonols, and anthocyanins in the wild type were assigned a value of 1.0, and their levels in mutant and transgenic lines were compared with those of the wild type in triplicate.

Transient transcription dual-luciferase assays

The ORF of *AP2m3* and the promoter regions of 25 PA pathway genes were cloned into pENTR/SD/D-TOPO and confirmed by sequencing. For mutation of the AT-rich motifs (TTTGTT or AACAAA) in the *MYBL2* promoter, mutated promoters in which AT-rich motifs M1–M5 were mutated into CCCCCC were cloned into pENTR/D/TOPO and confirmed by sequencing. The resulting pENTR-AP2m3 was subcloned into the modified destination vector p2GW7 by LR reaction to generate p2GW7-AP2m3. The resulting pENTR-promoter vectors containing individual promoters were subcloned into the modified destination vector p2GW7-LUC by LR reaction to generate p2GW7-promoter vectors (Karimi et al., 2002). The ORFs of *TT2*, *TT8*, *TTG1*, and *MYBL2* were cloned into p2GW7. Leaves of 4-week-old *Arabidopsis* seedlings were used for protoplast isolation as described previously (Yoo et al., 2007). The effector construct (p2GW7-gene) driven by the 35S promoter was co-transfected with each individual reporter construct (p2GW7-promoter) into *Arabidopsis* protoplasts as described previously (Yoo et al., 2007). A reference construct containing the *Renilla* luciferase gene driven by the 35S promoter was also co-transfected to measure transfection efficiency. Luciferase activities were measured using the dual-luciferase reporter assay system (Promega), and the firefly luciferase activity was calculated by normalizing against the *Renilla* luciferase activity in each transfection event. Data are presented as mean ± standard deviation of biological triplicates.

Yeast two-hybrid assays

The ORFs and different truncations of *AP2* and *MYBL2* were amplified and cloned into the gateway destination vector pGBKT7-DEST with a binding domain (Clontech, Mountain View, CA, USA). ORFs of *AP2* and *TT2*, *MYB5*, *TT8*, *GL3*, *EGL3*, *TTG1*, *TTG2*, *MYBL2*, *TT1*, *TT16*, and *STK* of the PA pathway were cloned into pGADT7-DEST with an activation domain (Clontech). Yeast strain AH109 cells were co-transformed with specific bait and prey constructs using the LiCl–polyethylene glycol method according to the manufacturer's instructions (Clontech). The transformants were grown on synthetic SD/−Trp/−Leu dropout medium and further selected on SD/−Trp/−Leu/−His/−Ade medium with 3-amino-1,2,4-triazole at 30°C for 7 days.

BiFC assays

The ORFs of *AP2m3*, *TT8*, *GL3*, and *EGL3* were cloned into the *Pac* I and *Spe* I restriction sites of the pBI-2YN-CAT vector. The ORFs of *MYBL2*, *TT2*, *MYB5*, *TT8*, *GL3*, *EGL3*, and *TTG1* and the C-terminal and N-terminal truncations of *MYBL2* were cloned into the *Pac* I and *Spe* I restriction sites of the pBI-2YC-CAT vector. *Agrobacterium* cells containing each construct were incubated at 28°C in Luria-Bertani medium with shaking at 200 rpm until the optical density value reached 0.6–0.8. *Agrobacterium* cells were then centrifuged for 10 min at 4000 rpm and resuspended in induction medium (10 mM 2-(N-Morpholino) ethane sulfonate buffer [pH 5.6], 10 mM $MgCl_2$, and 150 μM acetosyringone), then co-infiltrated into epidermal cells of young leaves of 4-week-old *N. benthamiana*. YFP fluorescence was detected 40–48 h after infiltration by laser-scanning confocal microscopy (Leica TCS SP5). Emission was collected at 520–550 nm for YFP and at 600–630 nm for mCherry.

CoIP assays

AP2m3 and *MYBL2* were cloned into modified pCAMBIA1302 vectors containing the 3×Myc tag and the 3×FLAG tag, respectively. *TT8*, *GL3*, and *EGL3* were cloned into a modified pCAMBIA1302 vector containing the 3×HA tag. All primers are listed in Supplementary Table 1. To verify the interaction of AP2 with MYBL2, 4-week-old *N. benthamiana* leaves were infiltrated with *A. tumefaciens* GV3101 harboring Pro35S:MYBL2-3×FLAG and Pro35S:AP2m3-3×Myc. To test the interaction of MYBL2 with TT8, GL3, and EGL3, GV3101 cells harboring Pro35S:MYBL2-3×FLAG combined with Pro35S:TT8-3×HA, Pro35S:GL3-3×HA, or Pro35S:EGL3-3×HA, respectively, were infiltrated into *N. benthamiana* leaves. These leaves were harvested 36–48 h after infiltration. Total proteins were extracted from leaves with coIP buffer (100 mM Tris–HCl, 300 mM NaCl, 2 mM EDTA, 10% glycerol, 1% Triton X-100, and 1% protease inhibitor cocktail [pH 7.5]). An anti-Myc tag antibody or anti-HA tag antibody (Abcam, Cambridge, UK) was added to protein extracts and incubated at 4°C for 3 h. Immuno-complexes captured by the beads were washed three times with coIP buffer.

ChIP assays

Wild-type *Arabidopsis* and transgenic *Arabidopsis* overexpressing AP2m3-Myc were grown at 23°C under 16-h light and 8-h dark conditions. Siliques of 3- to 5-day-old plants were cross-linked for 15 min in 1% formaldehyde by vacuum infiltration. The ChIP analysis was performed using an anti-Myc tag antibody (Abcam), and quantitative real-time PCR was performed using SYBR Green reagent (GeneStar) and the ABI 7500 Real-time Detection System (Applied Biosystems). Results are presented as the ratio of the amount of DNA immunoprecipitated from AP2m3-Myc samples to that of the wild type in triplicates. The *PP2A* and *UBC30* genes were used as negative controls.

ACCESSION NUMBERS

Sequence data in this article can be found at The Arabidopsis Information Resource under the following accession numbers: *AP2* (At4G36920), *TOE1* (At2G28550), *TOE2* (At5G60120), *TOE3* (At5G67180), *SMZ* (At3G54990), *SNZ* (At2G39250), *miR172a* (At2G28056), *UBQ10* (At4G05320), *PP2A* (At1G13320), *UBC30* (At5G56150), *CHS* (At5G13930), *CHI* (At3G55120), *CHIL* (At5G05270), *F3H* (At3G51240), *F3′H* (At5G07990), *DFR* (At5G42800), *ANS* (At4G22880), *ANR* (At1G61720), *TT12* (At3G59030), *TT19* (At5G17220), *AHA10* (At1G17260), *TT10* (At5G48100), *TT2* (At5G35550), *MYB5* (At3G13540), *TT8* (At4G09820), *GL3* (At5G41315), *EGL3* (At1G63650), *TTG1* (At5G24520), *MYBL2* (At1G71030), *TTG2* (At2G37260), *TT1* (At1G34790), *TT15* (At1G43620), *TT9* (At3G28430), *TT16* (At5G23260), and *STK* (At4G09960).

SUPPLEMENTAL INFORMATION

Supplemental information is available at *Plant Communications Online*.

FUNDING

This work was supported by grants from the National Natural Science Foundation of China (31870281 to W.J.) and the Agricultural Science and Technology Innovation Program (ASTIP-IAS10).

AUTHOR CONTRIBUTIONS

W.J. and Y.P. designed the research. W.J., Q.Y., J.L., and X.S. performed the analyses of proanthocyanidins, flavonols, and anthocyanins. W.J., Q.Y., and X.H. performed the transient transcriptional activity assay. J.Z. generated plants overexpressing the *AP2*-like miR172-target clade genes. W.J. and J.Z. performed the Y2H assay and ChIP assay. W.J. and Q.L. performed gene expression analysis, the BiFC assay, and the coIP assay. W.J. analyzed the data and interpreted the results. W.J. and Y.P. wrote the article.

ACKNOWLEDGMENTS

We thank Prof. John J. Harada (University of California, Davis) for providing the seeds of *ap2-5* and *ap2-6*, Prof. Loic Lepiniec (Institut National de la Recherche Agronomique [INRA], Versailles, France) for providing the seeds of *MYBL2* overexpression lines (H3 and H6), Prof. Lei Wang (Institute of Botany, Chinese Academy of Sciences, Beijing, China) for providing the pBI-2YC-CAT and pBI-2YN-CAT vectors, and Prof. Baichen Wang (Institute of Botany, Chinese Academy of Sciences, Beijing, China) for help with *in situ* hybridization. No conflict of interest is declared.

Received: August 25, 2023
Revised: November 2, 2023
Accepted: December 1, 2023
Published: December 5, 2023

REFERENCES

Appelhagen, I., Lu, G.H., Huep, G., Schmelzer, E., Weisshaar, B., and Sagasser, M. (2011). TRANSPARENT TESTA1 interacts with R2R3-MYB factors and affects early and late steps of flavonoid biosynthesis in the endothelium of *Arabidopsis thaliana* seeds. Plant J. **67**:406–419.

Aukerman, M.J., and Sakai, H. (2003). Regulation of flowering time and floral organ identity by a MicroRNA and its APETALA2-like target genes. Plant Cell **15**:2730–2741.

Baudry, A., Heim, M.A., Dubreucq, B., Caboche, M., Weisshaar, B., and Lepiniec, L. (2004). TT2, TT8, and TTG1 synergistically specify the expression of BANYULS and proanthocyanidin biosynthesis in *Arabidopsis thaliana*. Plant J. **39**:366–380.

Bowman, J.L., Smyth, D.R., and Meyerowitz, E.M. (1989). Genes directing flower development in Arabidopsis. Plant Cell **1**:37–52.

Bowman, J.L., Smyth, D.R., and Meyerowitz, E.M. (1991). Genetic interactions among floral homeotic genes of Arabidopsis. Development **112**:1–20.

Chen, X. (2004). A microRNA as a translational repressor of APETALA2 in Arabidopsis flower development. Science **303**:2022–2025.

Clough, S.J., and Bent, A.F. (1998). Floral dip: a simplified method for Agrobacterium-mediated transformation of *Arabidopsis thaliana*. Plant J. **16**:735–743.

Debeaujon, I., Nesi, N., Perez, P., Devic, M., Grandjean, O., Caboche, M., and Lepiniec, L. (2003). Proanthocyanidin-accumulating cells in Arabidopsis testa: regulation of differentiation and role in seed development. Plant Cell **15**:2514–2531.

Dinh, T.T., Girke, T., Liu, X., Yant, L., Schmid, M., and Chen, X. (2012). The floral homeotic protein APETALA2 recognizes and acts through an AT-rich sequence element. Development **139**:1978–1986.

Dixon, R.A., Xie, D.Y., and Sharma, S.B. (2005). Proanthocyanidins-a final frontier in flavonoid research? New Phytol. **165**:9–28.

Drews, G.N., Bowman, J.L., and Meyerowitz, E.M. (1991). Negative regulation of the Arabidopsis homeotic gene AGAMOUS by the APETALA2 product. Cell **65**:991–1002.

Dubos, C., Le Gourrierec, J., Baudry, A., Huep, G., Lanet, E., Debeaujon, I., Routaboul, J.M., Alboresi, A., Weisshaar, B., and Lepiniec, L. (2008). MYBL2 is a new regulator of flavonoid biosynthesis in *Arabidopsis thaliana*. Plant J. **55**:940–953.

Gonzalez, A., Brown, M., Hatlestad, G., Akhavan, N., Smith, T., Hembd, A., Moore, J., Montes, D., Mosley, T., Resendez, J., et al. (2016). TTG2 controls the developmental regulation of seed coat tannins in Arabidopsis by regulating vacuolar transport steps in the proanthocyanidin pathway. Dev. Biol. **419**:54–63.

Gou, J.Y., Felippes, F.F., Liu, C.J., Weigel, D., and Wang, J.W. (2011). Negative regulation of anthocyanin biosynthesis in Arabidopsis by a miR156-targeted SPL transcription factor. Plant Cell **23**:1512–1522.

Huang, Z., Shi, T., Zheng, B., Yumul, R.E., Liu, X., You, C., Gao, Z., Xiao, L., and Chen, X. (2017). APETALA2 antagonizes the transcriptional activity of AGAMOUS in regulating floral stem cells in *Arabidopsis thaliana*. New Phytol. **215**:1197–1209.

Ishida, T., Hattori, S., Sano, R., Inoue, K., Shirano, Y., Hayashi, H., Shibata, D., Sato, S., Kato, T., Tabata, S., et al. (2007). Arabidopsis TRANSPARENT TESTA GLABRA2 is directly regulated by R2R3 MYB transcription factors and is involved in regulation of GLABRA2 transcription in epidermal differentiation. Plant Cell **19**:2531–2543.

Jiang, W., Yin, Q., Wu, R., Zheng, G., Liu, J., Dixon, R.A., and Pang, Y. (2015). Role of a chalcone isomerase-like protein in flavonoid biosynthesis in *Arabidopsis thaliana*. J. Exp. Bot. **66**:7165–7179.

Jiang, W.B., Huang, H.Y., Hu, Y.W., Zhu, S.W., Wang, Z.Y., and Lin, W.H. (2013). Brassinosteroid regulates seed size and shape in Arabidopsis. Plant Physiol. **162**:1965–1977.

Joanisse, G.D., Bradley, R.L., Preston, C.M., and Bending, G.D. (2009). Sequestration of soil nitrogen as tannin-protein complexes may improve the competitive ability of sheep laurel (*Kalmia angustifolia*) relative to black spruce (*Picea mariana*). New Phytol. **181**:187–198.

Jofuku, K.D., den Boer, B.G., Van Montagu, M., and Okamuro, J.K. (1994). Control of Arabidopsis flower and seed development by the homeotic gene APETALA2. Plant Cell **6**:1211–1225.

Jofuku, K.D., Omidyar, P.K., Gee, Z., and Okamuro, J.K. (2005). Control of seed mass and seed yield by the floral homeotic gene APETALA2. Proc. Natl. Acad. Sci. USA **102**:3117–3122.

Jung, J.H., Lee, S., Yun, J., Lee, M., and Park, C.M. (2014). The miR172 target TOE3 represses AGAMOUS expression during Arabidopsis floral patterning. Plant Sci. **215–216**:29–38.

Kang, Y.H., Kirik, V., Hulskamp, M., Nam, K.H., Hagely, K., Lee, M.M., and Schiefelbein, J. (2009). The MYB23 gene provides a positive feedback loop for cell fate specification in the Arabidopsis root epidermis. Plant Cell **21**:1080–1094.

Karimi, M., Inzé, D., and Depicker, A. (2002). GATEWAY vectors for Agrobacterium-mediated plant transformation. Trends Plant Sci. **7**:193–195.

Koshino-Kimura, Y., Wada, T., Tachibana, T., Tsugeki, R., Ishiguro, S., and Okada, K. (2005). Regulation of CAPRICE transcription by MYB proteins for root epidermis differentiation in Arabidopsis. Plant Cell Physiol. **46**:817–826.

Kouchi, H., and Hata, S. (1993). Isolation and characterization of novel nodulin cDNAs representing genes expressed at early stages of soybean nodule development. Mol. Gen. Genet. **238**:106–119.

Krogan, N.T., Hogan, K., and Long, J.A. (2012). APETALA2 negatively regulates multiple floral organ identity genes in Arabidopsis by recruiting the co-repressor TOPLESS and the histone deacetylase HDA19. Development **139**:4180–4190.

Kunst, L., Klenz, J.E., Martinez-Zapater, J., and Haughn, G.W. (1989). *AP2* gene determines the identity of perianth organs in flowers of *Arabidopsis thaliana*. Plant Cell **1**:1195–1208.

Lees, G.L. (1992). Condensed tannins in some forage legumes: their role in the prevention of ruminant pasture bloat. Basic Life Sci. **59**:915–934.

Lepiniec, L., Debeaujon, I., Routaboul, J.M., Baudry, A., Pourcel, L., Nesi, N., and Caboche, M. (2006). Genetics and biochemistry of seed flavonoids. Annu. Rev. Plant Biol. **57**:405–430.

Li, M., He, X., La Hovary, C., Zhu, Y., Dong, Y., Liu, S., Xing, H., Liu, Y., Jie, Y., Ma, D., et al. (2022). A *de novo* regulation design shows an effectiveness in altering plant secondary metabolism. J. Adv. Res. **37**:43–60.

Li, P., Dong, Q., Ge, S., He, X., Verdier, J., Li, D., and Zhao, J. (2016). Metabolic engineering of proanthocyanidin production by repressing the isoflavone pathways and redirecting anthocyanidin precursor flux in legume. Plant Biotechnol. J. **14**:1604–1618.

Liu, X., Dinh, T.T., Li, D., Shi, B., Li, Y., Cao, X., Guo, L., Pan, Y., Jiao, Y., and Chen, X. (2014). AUXIN RESPONSE FACTOR 3 integrates the functions of AGAMOUS and APETALA2 in floral meristem determinacy. Plant J. **80**:629–641.

Mathieu, J., Yant, L.J., Mürdter, F., Küttner, F., and Schmid, M. (2009). Repression of flowering by the miR172 target SMZ. PLoS Biol. **7**, e1000148.

Matsui, K., Umemura, Y., and Ohme-Takagi, M. (2008). AtMYBL2, a protein with a single MYB domain, acts as a negative regulator of anthocyanin biosynthesis in Arabidopsis. Plant J. **55**:954–967.

Mizzotti, C., Ezquer, I., Paolo, D., Rueda-Romero, P., Guerra, R.F., Battaglia, R., Rogachev, I., Aharoni, A., Kater, M.M., Caporali, E., and Colombo, L. (2014). SEEDSTICK is a master regulator of development and metabolism in the Arabidopsis seed coat. PLoS Genet. **10**, e1004856.

Nesi, N., Debeaujon, I., Jond, C., Stewart, A.J., Jenkins, G.I., Caboche, M., and Lepiniec, L. (2002). The TRANSPARENT TESTA16 locus encodes the ARABIDOPSIS BSISTER MADS domain protein and is required for proper development and pigmentation of the seed coat. Plant Cell **14**:2463–2479.

Nesi, N., Jond, C., Debeaujon, I., Caboche, M., and Lepiniec, L. (2001). The Arabidopsis TT2 gene encodes an R2R3 MYB domain protein that acts as a key determinant for proanthocyanidin accumulation in developing seed. Plant Cell **13**:2099–2114.

Ó'Maoiléidigh, D.S., van Driel, A.D., Singh, A., Sang, Q., Le Bec, N., Vincent, C., de Olalla, E.B.G., Vayssières, A., Romera Branchat, M., Severing, E., et al. (2021). Systematic analyses of the MIR172 family members of Arabidopsis define their distinct roles in regulation of APETALA2 during floral transition. PLoS Biol. **19**, e3001043.

Ohto, M.A., Fischer, R.L., Goldberg, R.B., Nakamura, K., and Harada, J.J. (2005). Control of seed mass by APETALA2. Proc. Natl. Acad. Sci. USA **102**:3123–3128.

Ohto, M.A., Floyd, S.K., Fischer, R.L., Goldberg, R.B., and Harada, J.J. (2009). Effects of APETALA2 on embryo, endosperm, and seed coat development determine seed size in Arabidopsis. Sex. Plant Reprod. **22**:277–289.

Pourcel, L., Routaboul, J.M., Kerhoas, L., Caboche, M., Lepiniec, L., and Debeaujon, I. (2005). TRANSPARENT TESTA10 encodes a laccase-like enzyme involved in oxidative polymerization of flavonoids in Arabidopsis seed coat. Plant Cell **17**:2966–2980.

Prior, R.L., and Gu, L. (2005). Occurrence and biological significance of proanthocyanidins in the American diet. Phytochemistry **66**:2264–2280.

Qi, T., Song, S., Ren, Q., Wu, D., Huang, H., Chen, Y., Fan, M., Peng, W., Ren, C., and Xie, D. (2011). The Jasmonate-ZIM-domain proteins interact with the WD-Repeat/bHLH/MYB complexes to regulate Jasmonate-mediated anthocyanin accumulation and trichome initiation in *Arabidopsis thaliana*. Plant Cell **23**:1795–1814.

Ripoll, J.J., Roeder, A.H.K., Ditta, G.S., and Yanofsky, M.F. (2011). A novel role for the floral homeotic gene APETALA2 during Arabidopsis fruit development. Development **138**:5167–5176.

Ryu, K.H., Kang, Y.H., Park, Y.H., Hwang, I., Schiefelbein, J., and Lee, M.M. (2005). The WEREWOLF MYB protein directly regulates CAPRICE transcription during cell fate specification in the Arabidopsis root epidermis. Development **132**:4765–4775.

Sagasser, M., Lu, G.H., Hahlbrock, K., and Weisshaar, B. (2002). *A. thaliana* TRANSPARENT TESTA 1 is involved in seed coat development and defines the WIP subfamily of plant zinc finger proteins. Genes Dev. **16**:138–149.

Sawa, S. (2002). Overexpression of the *AtmybL2* gene represses trichome development in Arabidopsis. DNA Res. **9**:31–34.

Schwab, R., Palatnik, J.F., Riester, M., Schommer, C., Schmid, M., and Weigel, D. (2005). Specific effects of microRNAs on the plant transcriptome. Dev. Cell **8**:517–527.

Sharma, S.B., and Dixon, R.A. (2005). Metabolic engineering of proanthocyanidins by ectopic expression of transcription factors in *Arabidopsis thaliana*. Plant J. **44**:62–75.

Song, S.K., Ryu, K.H., Kang, Y.H., Song, J.H., Cho, Y.H., Yoo, S.D., Schiefelbein, J., and Lee, M.M. (2011). Cell fate in the Arabidopsis root epidermis is determined by competition between WEREWOLF and CAPRICE. Plant Physiol. **157**:1196–1208.

Thévenin, J., Dubos, C., Xu, W., Le Gourrierec, J., Kelemen, Z., Charlot, F., Nogué, F., Lepiniec, L., and Dubreucq, B. (2012). A new system for fast and quantitative analysis of heterologous gene expression in plants. New Phytol. **193**:504–512.

Verdier, J., Zhao, J., Torres-Jerez, I., Ge, S., Liu, C., He, X., Mysore, K.S., Dixon, R.A., and Udvardi, M.K. (2012). MtPAR MYB transcription factor acts as an on switch for proanthocyanidin biosynthesis in *Medicago truncatula*. Proc. Natl. Acad. Sci. USA **109**:1766–1771.

Western, T.L., Burn, J., Tan, W.L., Skinner, D.J., Martin-McCaffrey, L., Moffatt, B.A., and Haughn, G.W. (2001). Isolation and characterization of mutants defective in seed coat mucilage secretory cell development in Arabidopsis. Plant Physiol. **127**:998–1011.

Wollmann, H., Mica, E., Todesco, M., Long, J.A., and Weigel, D. (2010). On reconciling the interactions between APETALA2, miR172 and AGAMOUS with the ABC model of flower development. Development **137**:3633–3642.

Würschum, T., Gross-Hardt, R., and Laux, T. (2006). APETALA2 regulates the stem cell niche in the Arabidopsis shoot meristem. Plant Cell **18**:295–307.

Xie, Y., Tan, H., Ma, Z., and Huang, J. (2016). DELLA proteins promote anthocyanin biosynthesis via sequestering MYBL2 and JAZ suppressors of the MYB/bHLH/WD40 complex in *Arabidopsis thaliana*. Mol. Plant **9**:711–721.

Xu, W., Bobet, S., Le Gourrierec, J., Grain, D., De Vos, D., Berger, A., Salsac, F., Kelemen, Z., Boucherez, J., Rolland, A., et al. (2017). TRANSPARENT TESTA 16 and 15 act through different mechanisms to control proanthocyanidin accumulation in Arabidopsis testa. J. Exp. Bot. **68**:2859–2870.

Xu, W., Dubos, C., and Lepiniec, L. (2015). Transcriptional control of flavonoid biosynthesis by MYB-bHLH-WDR complexes. Trends Plant Sci. **20**:176–185.

Xu, W., Grain, D., Bobet, S., Le Gourrierec, J., Thévenin, J., Kelemen, Z., Lepiniec, L., and Dubos, C. (2014). Complexity and robustness of the flavonoid transcriptional regulatory network revealed by

comprehensive analyses of MYB-bHLH-WDR complexes and their targets in Arabidopsis seed. New Phytol. **202**:132–144.

Yant, L., Mathieu, J., Dinh, T.T., Ott, F., Lanz, C., Wollmann, H., Chen, X., and Schmid, M. (2010). Orchestration of the floral transition and floral development in Arabidopsis by the bifunctional transcription factor APETALA2. Plant Cell **22**:2156–2170.

Yoo, S.D., Cho, Y.H., and Sheen, J. (2007). Arabidopsis mesophyll protoplasts: a versatile cell system for transient gene expression analysis. Nat. Protoc. **2**:1565–1572.

Yumul, R.E., Kim, Y.J., Liu, X., Wang, R., Ding, J., Xiao, L., and Chen, X. (2013). POWERDRESS and diversified expression of the MIR172 gene family bolster the floral stem cell network. PLoS Genet. **9**, e1003218.

Zhao, L., Kim, Y., Dinh, T.T., and Chen, X. (2007). miR172 regulates stem cell fate and defines the inner boundary of APETALA3 and PISTILLATA expression domain in Arabidopsis floral meristems. Plant J. **51**:840–849.

Zhu, H.F., Fitzsimmons, K., Khandelwal, A., and Kranz, R.G. (2009). CPC, a single-repeat R3 MYB, is a negative regulator of anthocyanin biosynthesis in Arabidopsis. Mol. Plant **2**:790–802.

Zimmermann, I.M., Heim, M.A., Weisshaar, B., and Uhrig, J.F. (2004). Comprehensive identification of *Arabidopsis thaliana* MYB transcription factors interacting with R/B-like BHLH proteins. Plant J. **40**:22–34.